



## FREE VIBRATION ANALYSIS OF GRAVITY DAM SECTIONS USING ISOGEOMETRIC ANALYSIS

<sup>1</sup>RODNNY JESUS MENDOZA FAKHYE, <sup>2</sup>ROBERTO DALLEDONE MACHADO, MATEUS RAUEN<sup>3</sup>, MARCOS ARNDT<sup>4</sup>

<sup>1</sup>Asstt. Prof., Federal Technological University of Paraná, Brazil

<sup>2</sup>Assoc. Prof., Federal University of Paraná, Brazil

<sup>3</sup>Graduate Student, Federal University of Paraná, Brazil

<sup>4</sup>Asstt. Prof., Federal Technological University of Paraná, Brazil

E-mail: <sup>1</sup>[rodny@utfpr.edu.br](mailto:rodny@utfpr.edu.br), <sup>2</sup>[rdm@ufpr.br](mailto:rdm@ufpr.br), <sup>3</sup>[mateusrauen@gmail.com](mailto:mateusrauen@gmail.com), <sup>4</sup>[arndt@ufpr.br](mailto:arndt@ufpr.br)

### ABSTRACT

*Isogeometric Analysis (IGA) is a numerical approach that allows the discretization and analysis of continuous medium using the approximation functions generated in the construction of digital models or Computer Aided Design (CAD) models. In the present study, first IGA is applied in the study of two-dimensional linear elasticity problems and then to free vibration problems in plane stress and a cross section of a gravity concrete dam in plane strain state. Numerical tests are presented to show the performance and discuss future applications.*

**Keywords:** *Isogeometric Analysis; plane stress, plane strain; free vibrations*

### 1. INTRODUCTION

Among the numerical methods used in modeling and analysis of structures, the Finite Element Method (FEM) [1]–[3] is one of the most widely used and is widely popular among engineers and designers.

Nowadays in the development phase of a project, the geometry of the structure is developed in a CAD (Computer Aided Design) system. Then from this digital model the finite element mesh is generated and will be used in the analysis phase of the structure, whether static or dynamic, placing an appropriate number of nodes and elements in order to obtain both: a good approximation and a good geometric precision.

In the classical formulation of FEM, polynomial interpolation functions are used both in the evaluation of the unknowns as in the geometry approximation. The functions normally employed (Ex. Lagrange Polynomials) are different from those used by CAD software. Cottrell et al. [4] indicates that the generation of local and global finite element matrices can consume up to 60% of

the time used for modeling and analysis. Interpolations made by the finite element basis functions are not integrated with those used in the generation of the solid model. It follows, therefore, that the interpolation process is duplicated, since it occurs in two different ways for the same problem: First, the generation of the CAD model, and second in the matrix generation of the FEM [5].

The Isogeometric Analysis (IGA) is a recent approach where the approximation functions are those traditionally used in computer graphics, commonly known as NURBS (Non Uniform Rational B-Splines).

An advantage of this approach is the direct communication between CAD environments and analysis environment enabling an optimization of time in pre-processing and analysis phases. Still, as IGA allows to work in the "exact" geometry making possible to eliminate imperfections and modeling errors by providing more accurate solutions for certain problems [5].

Cottrell et al. [6] also found that IGA shows better dynamic response than conventional finite

element formulation in the frequency spectrum. Discontinuities in accuracy appear only in the region of higher frequency of vibration problems. This feature can be decisive in wave propagation studies.

Structural Health Monitoring (SHM) [7] considers the analysis of vibrations in dams as a fundamental problem for the design and construction of dams. Excessive vibrations may generate damage, defined as changes in the material, geometric shapes, including changes in boundary conditions or support, which can adversely affect the performance of the structure [8].

Considering this, the application of IGA on vibration problems of dams is an interesting and promising application because the use of CAD environments is an established practice in design of new dams and the documentation of dams built in pre-digital era.

The use of digital geometric information generated in CAD systems of a dam already built or in design stage, would be a significant contribution avoiding additional modeling steps and will contribute to improving the safety of these structures. Figure 1 show a tridimensional CAD model of the Itaipu dam in Brazil.

## 2. ISOGOMETRIC ANALYSIS

Since the introduction of the basic concepts of IGA by Hughes et al. [5], several studies have been conducted to extend its application to different fields of computational mechanics. In those studies, IGA has shown similar or superior performance compared to FEM, and there was found a precision gain in the treatment of certain problems such as turbulence, nonlinear analysis of shell type structures, shape optimization and aerodynamics [9]–[12].



Figure 1: Tridimensional CAD model of a section of the Itaipu dam, Brazil, retrieved from the original documentation [13]

It is also known that finite elements with low order formulations suffer the locking phenomenon in flexural dominated problems. The FEM solution with high order functions can be expensive from the computational point of view. The mathematical characteristics of NURBS functions are expected to give IGA a more efficient performance [4].

### 2.1 Basics of IGA

In the FEM context, a mesh of finite elements is a discretization of the domain of analysis, which is divided by several subdomains that are the elements. However, because of mapping conditions an element has two representations, one in the parametric domain and the other in the physical domain. The elements are usually defined by their coordinates and nodal degrees of freedom that are usually the values of the basis functions at the nodes. These basis functions are also called shape functions [14].

In IGA there are two mesh definitions: the control mesh and the physical mesh. Control points define the control mesh, and the control mesh interpolates the control points. The appearance of the control mesh is similar to a finite element mesh, but there is no direct relationship between them. The unknowns of the problem are the degrees of freedom located at the control points [4].

NURBS functions are constructed from a set of points in parameter space called knots, normally grouped in vectors. These knot vectors define the geometry of the physical network and have not necessarily associated to degrees of freedom.

In linear space, an element within the IGA is defined as the domain between two separate

control points. Similarly, it is possible to generalize this concept to two-dimensional and three-dimensional spaces [14].

Figure 6 schematically illustrates the relationship between the geometric and parametric domains in a IGA based code. In this figure there are shown: the physical domain, the parametric domain and the domain corresponding to an isogeometric element. The description of the basis functions and the numerical formulation of the problem will be shown below.

### 2.2 Knot Vectors and Basis Functions

The knot vector is a non-decreasing set of coordinates in parameter space given by  $\Xi = \{\xi_1, \xi_2, \dots, \xi_{n+p+1}\}$  where  $\xi_i$  is the  $i$ -th knot,  $p$  is the polynomial degree and  $n$  is the number of basis functions used to generate the curve.

Knot vectors can be equally spaced (uniform) or not (non-uniform). A single coordinate of a knot may be repeated taking the same value, this feature is called multiplicity.

Basis functions are directly influenced by knot vectors. An open vector is one in which the control points at the beginning and the end are repeated  $p + 1$  times. Open vectors are the standard in CAD environments [15].

The basis functions are built recursively starting with a polynomial degree  $p = 0$ .

The basis functions of a B-spline parametric curve are defined recursively. For  $p=0$ :

$$N_{i,0} = \begin{cases} 1 & \text{if } \xi_i \leq \xi < \xi_{i+1} \\ 0 & \text{else} \end{cases} \quad (1)$$

For greater orders ( $p = 1, 2, 3, \dots$ ), we have:

$$N_{i,p}(\xi) = \frac{\xi - \xi_i}{\xi_{i+p} - \xi_i} N_{i,p-1}(\xi) + \frac{\xi_{i+p+1} - \xi}{\xi_{i+p+1} - \xi_{i+1}} N_{i+1,p-1}(\xi) \quad (2)$$

The derivatives of the B-spline functions are also defined recursively [16].

### 2.3 B-Splines curves and surfaces

B-Spline curves are constructed from the linear combination of the basis functions B-Spline and control points. For  $n$  basis functions with  $n$  control points  $\mathbf{P}_i$ , the polynomial equation of a B-spline curve is given by:

$$\mathbf{C}(\xi) = \sum_{i=1}^n N_{i,p}(\xi) \mathbf{P}_i \quad (3)$$

Given a control mesh  $\{\mathbf{P}_{i,j}\}, i=1,2,\dots,n; j=1,2,\dots,m$  with polynomial orders  $p$  and  $q$  and knots vectors  $\Xi = \{\xi_1, \xi_2, \dots, \xi_{n+p+1}\}$  and  $H = \{\eta_1, \eta_2, \dots, \eta_{m+p+1}\}$ . Using tensor product described in Equation (4) a B-Spline surface is obtained.

$$\mathbf{S}(\xi, \eta) = \sum_{i=1}^n \sum_{j=1}^m N_{i,p}(\xi) M_{j,q}(\eta) \mathbf{P}_{i,j} \quad (4)$$

Figure 2 shows a quadratic B-spline tensor product surface. In this case  $\Xi = \{0, 0, 0, .5, 1, 1, 1\}$  and  $H = \{0, 0, 0, 1, 1, 1\}$ .

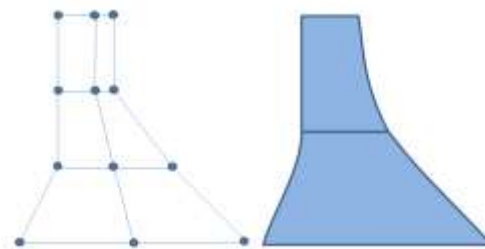


Figure 2: Control Mesh and Physical mesh for a quadratic surface with two isogeometric elements.

### 2.4 NURBS Curves and surfaces

A NURBS curve can be obtained by the projective transformation of a B-spline curve [4]. Also we can think a NURBS curve as a parametric rational B-Spline curve with a non-uniform knot vector.

Equation (5) represents a NURBS curve of  $p$  degree, control points  $\mathbf{P}_i$ , with knot vector  $\Xi$  and weights  $w_i$ .

$$\mathbf{C}(\xi) = \frac{\sum_{i=0}^n N_{i,p}(\xi) w_i \mathbf{P}_i}{\sum_{j=0}^n N_{j,p}(\xi) w_j} \quad (5)$$

These rational curves enable efficient computational processing and compact storage of data[16]. The use of open knot vectors allows the insertion of degrees of freedom at domain ends. As rational functions, NURBS curves allow the modeling of conic and quadric surfaces. Figure 3 shows NURBS curves obtained this way with  $\xi = [0, 0, 0, 1, 2, 3, 3, 3]$  and  $w = [1, 1, w, 1]$ .

### 3. IGA APPLIED IN TWO-DIMENSIONAL LINEAR ELASTICITY PROBLEMS

#### 3.1 Problem Description

Linear elasticity problems can be formulated through the differential equation of equilibrium.

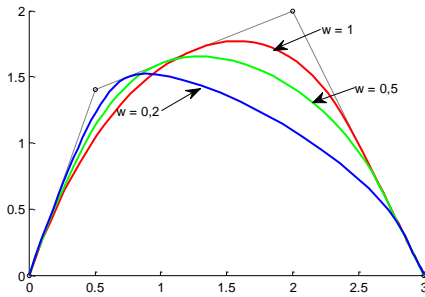


Figure 3: Quadratic NURBS curves

This equation in indicial notation became:

$$\sigma_{ij,j} + f_i = 0 \quad \text{in } \Omega \quad (6)$$

Subjected to the following boundary conditions:

$$\sigma_{ij} n_j = h_i \quad \text{in } \Gamma_\sigma \quad (7)$$

$$u_i = \bar{u} \quad \text{in } \Gamma_u \quad (8)$$

Equation (7) represent the natural boundary conditions or Neumann conditions and Equation (8) represent the essential boundary conditions or Dirichlet conditions. The set of Equations (6), (7) and (8) represent the static equilibrium of the body under study, with the support conditions and surface tensions.

For a linear elastic solid generalized Hooke's Law is given by:

$$\sigma_{ij} = C_{ijkl} \varepsilon_{ij} \quad (9)$$

Where  $C_{ijkl}$  are the elastic coefficients or the constitutive relationship and  $\varepsilon_{ij}$  is the infinitesimal deformations tensor.

According to [3], the weak form of the linear elasticity problem has the form:

$$\int_{\Omega} \hat{\sigma}_{ij} w_{i,j} d\Omega = \int_{\Omega} f_i w_i d\Omega + \int_{\Gamma_\sigma} h_i w_i d\Gamma_\sigma \quad (10)$$

Where  $\hat{\sigma}_{ij}$  is an approximate solution of the stress field and  $w$  is the weight function that minimizes the residual. Approximating the displacement field with a function like:

$$\hat{\mathbf{u}} = \sum_{k=1}^m N_k \mathbf{u}_k \quad (11)$$

Where  $N_k$  are the NURBS basis functions and  $\mathbf{u}_k$  represents the control point displacements. Applying the Galerkin method we obtain:

$$\sum_{k=1}^m \left( \int_{\Omega} \mathbf{B}^T \mathbf{C} \mathbf{B} d\Omega \right) \hat{\mathbf{u}}_k = \int_{\Omega} \mathbf{N} \mathbf{f} d\Omega + \int_{\Gamma_\sigma} \mathbf{N} \mathbf{h} d\Gamma_\sigma \quad (12)$$

Where  $\mathbf{B}$  is the NURBS basis functions derivatives matrix,  $\mathbf{C}$  is the constitutive matrix,  $\mathbf{N}$  is the NURBS basis functions matrix,  $\mathbf{f}$  represents the body forces and  $\mathbf{h}$  the surface tensions.

Equation (12) represents the algebraic system to be solved and the system stiffness matrix is:

$$\mathbf{K} = \sum_{k=1}^m \left( \int_{\Omega} \mathbf{B}^T \mathbf{C} \mathbf{B} d\Omega \right) \hat{\mathbf{u}}_k \quad (13)$$

#### 3.2 Numerical Applications

In order to test the IGA formulation, a Matlab® script was implemented following some of the guidelines described in [17]. The following applications aim to show the capabilities of the method.

### 3.2.1 Square plate under uniform axial stress

This problem has already an analytical well known solution and is presented as a basic test of the algorithm.

Figure 7 shows a rectangular plate under axial traction  $T_x$  in the  $x$  direction. According to [18] the analytical solution for the plane stress problem is:  $\sigma_x = T_x$ ,  $\sigma_y = 0$ ,  $u_x = T_x x / E$  and  $u_y = \nu u_x = \nu T_x x / E$ ; where  $E$  is the elasticity modulus of elasticity and  $\nu$  is the Poisson's ratio.

Considering:  $E = 105 \text{ N/mm}^2$ ,  $T_x = 10 \text{ N/mm}^2$ ,  $\nu = 0.3$  and the dimensions indicated, the analytical solution provides:  $u_x = 4 \times 10^{-4} \text{ mm}$  and  $u_y = 1.2 \times 10^{-5} \text{ mm}$ . Taking into account the symmetry of the problem only a quarter of the plate was analyzed. The analytical responses for stress and deformation were obtained with a single bi-quadratic isogeometric, as illustrated in Figure 7.

## 4. FREE UNDAMPED VIBRATION PROBLEMS WITH IGA

According to [19], a structure is subjected to free undamped vibrations when it is disturbed from its static equilibrium position and then allowed to vibrate without any external dynamic excitation without considering energy loses from dumping. Thus, the responses obtained by the free vibration analysis are the natural vibration frequencies and mode shapes.

### 4.1 Problem Description

Free undamped vibration problems in linear elasticity may be represented as a generalized eigenvalue problem [1], [2]:

$$(\mathbf{K} - \lambda \mathbf{M}) \mathbf{\Delta} = \mathbf{0} \quad (14)$$

Where  $\mathbf{\Delta}$  represent the eigenvector matrix that represents the plane vibration shape modes,  $\lambda$  is the square of the angular frequency ( $\omega$ ).  $\mathbf{K}$  is the stiffness matrix described in Equation (13) and  $\mathbf{M}$  is the consistent mass matrix calculated by:

$$\mathbf{M} = \int_{\Omega} \rho \mathbf{N}_j^T \mathbf{N}_k d\Omega \quad (15)$$

The matrices  $\mathbf{N}_j$  and  $\mathbf{N}_k$  are the NURBS basis matrices and  $\rho$  stands for the material density.

The solution of the generalized eigenvalue problem is the dynamic response of the structure.

### 4.2 Free Vibration of a Cantilever Beam

The cantilever beam represented in Figure 4 will be analyzed as a free vibration problem.



Figure 4: Cantilever beam and cross section for the free vibration problem

Considering the following dimensions  $L = 0.8$  meters,  $h = 10 \text{ cm}$ ,  $b = 1 \text{ cm}$  and elasticity modulus  $E = 200 \text{ GPa}$  and  $\nu = 0.3$ .

Table 1 shows the results for the free vibration frequencies for the first six modes of vibration and its comparison with the ANSYS® FEM solution using 1480 rectangular quadratic elements taken as reference. Relative difference between IGA and FEM solutions are showed in Table 2.

### 4.3 Concrete Gravity Dam Section

Now we show the results obtained for a plane strain state problem plan, which aims to determine the natural frequency and vibrational shape modes of the structure.

We consider plane strain state when the strain state at a material point is such that the only non-zero strain components act in one plane only. This hypothesis can be adopted for the analysis of a cross section of a dam, where the cross-section analyzed is contained within the dam mass [20]. So we considered a generic section of a gravity concrete dam whose dimensions are shown in Figure 5. Considering the base as fixed and the physical properties of the material are defined by elasticity modulus  $E = 21 \text{ GPa}$ ,  $\nu = 0.2$  and  $\rho = 25 \text{ kN/m}^3$ .

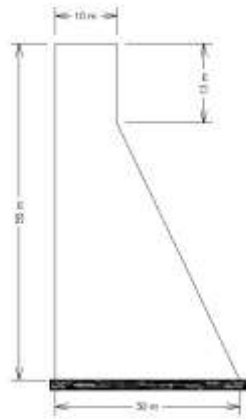


Figure 5: Generic cross section of a concrete gravity dam with fixed base

shows the results for the free vibration frequencies for the first six modes of vibration and its comparison with the ANSYS® FEM solution using 1480 rectangular quadratic elements taken as reference. Relative difference between IGA and FEM solutions are showed in Table 2.

## 5. FINAL DISCUSSION AND CONCLUSIONS

The study of eigenvectors problems such as vibration problems, allows to show a satisfactory performance of NURBS as approximation functions.

The results of this study are indicative that IGA can be successfully applied to structures and dam vibration problems. Literature [4]–[6] indicates that IGA has advantages from the point of view of vibration analysis, this may allow more accurate wave propagation in dam analysis.

Another important feature of IGA is that it make possible the use the recovered models of already built structures like dams, having great potential for future applications. Future works may include fluid-structure interaction and non-linear constitutive rules.

## ACKNOWLEDGEMENTS

The support of the Technological Park of Itaipu (PTI) and the Center for Advanced Studies in Dam Safety (CEASB) are gratefully acknowledged.

## REFERENCES

1. K. J. Bathe, *Finite element procedures*. New Jersey: Prentice Hall, 2006.

2. T. J. R. Hughes, *The Finite Element Method*. Mineola, NY: Dover, 2000.
3. J. N. Reddy, *An Introduction to the Finite Element Method*. Highstown: McGraw - Hill, 1993.
4. J. A. Cottrell, T. J. R. Hughes, and Y. Bazilevs, *Isogeometric Analysis: Toward Integration of CAD and FEA*, 1st ed. Chichester: John Wiley & Sons, 2009.
5. T. J. R. Hughes, J. A. Cottrell, and Y. Bazilevs, "Isogeometric analysis: CAD, finite elements, NURBS, exact geometry and mesh refinement," *Comput. Methods Appl. Mech. Eng.*, vol. 194, no. 39–41, pp. 4135–4195, 2005.
6. J. A. Cottrell, A. Reali, Y. Bazilevs, and T. J. R. Hughes, "Isogeometric analysis of structural vibrations," *Comput. Methods Appl. Mech. Eng.*, vol. 195, no. 41–43, pp. 5257–5296, 2006.
7. D. Balageas, C.-P. Fritzen, and A. Gemes, Eds., *Structural Health Monitoring*. London, UK: ISTE, 2006.
8. C. R. Farrar and K. Worden, "An introduction to structural health monitoring," *Philos. Trans. R. Soc. A Math. Phys. Eng. Sci.*, vol. 365, no. 1851, pp. 303–315, Feb. 2007.
9. Y. Bazilevs, V. M. Calo, J. A. Cottrell, T. J. R. Hughes, A. Reali, and G. Scovazzi, "Variational multiscale residual-based turbulence modeling for large eddy simulation of incompressible flows," *Comput. Methods Appl. Mech. Eng.*, vol. 197, no. 1–4, pp. 173–201, 2007.
10. D. J. Benson, Y. Bazilevs, M. C. Hsu, and T. J. R. Hughes, "Isogeometric shell analysis: The Reissner–Mindlin shell," *Comput. Methods Appl. Mech. Eng.*, vol. 199, no. 5–8, pp. 276–289, 2010.
11. J. Kiendl, R. Schmidt, R. Wüchner, and K.-U. Bletzinger, "Isogeometric shape optimization of shells using semi-analytical sensitivity analysis and sensitivity weighting," *Comput. Methods Appl. Mech. Eng.*, vol. 274, pp. 148–167, 2014.
12. S. Cho and S. H. Ha, "Isogeometric shape design optimization: Exact geometry and

- enhanced sensitivity,” *Struct. Multidiscip. Optim.*, vol. 38, no. 1, pp. 53–70, 2009.
13. CEASB, *Acervo técnico do CEASB*. Itaipu Binacional: Centro de Estudos Avançados em Segurança de Barragens, 2015.
  14. J. A. Cottrell, T. J. R. Hughes, and A. Reali, “Studies of refinement and continuity in isogeometric structural analysis,” *Comput. Methods Appl. Mech. Eng.*, vol. 196, no. 41–44, pp. 4160–4183, 2007.
  15. T. J. R. Hughes, J. A. Cottrell, and Y. Bazilevs, “Isogeometric analysis: CAD, finite elements, NURBS, exact geometry and mesh refinement,” *Comput. Methods Appl. Mech. Eng.*, vol. 194, no. 39–41, pp. 4135–4195, 2005.
  16. L. Piegl and W. Tiller, *The NURBS book*. Berlin: Springer Verlag, 1997.
  17. V. P. Nguyen, C. Anitescu, S. P. A. A. Bordas, and T. Rabczuk, “Isogeometric analysis: An overview and computer implementation aspects,” *Math. Comput. Simul.*, vol. 117, pp. 1–114, 2015.
  18. C. Felippa, “Introduction to Finite Element Methods,” in *Introduction to Finite Element Methods*, University of Colorado, 2004, p. Capítulo 27.
  19. A. K. Chopra, *Dynamics of structures: theory and applications to earthquake engineering*. Upper Saddle River, NJ: Pearson/Prentice Hall, 2012.
  20. R. B. Jansen, *Advanced dam engineering for design, construction, and rehabilitation*. Springer Science & Business Media, 2012.

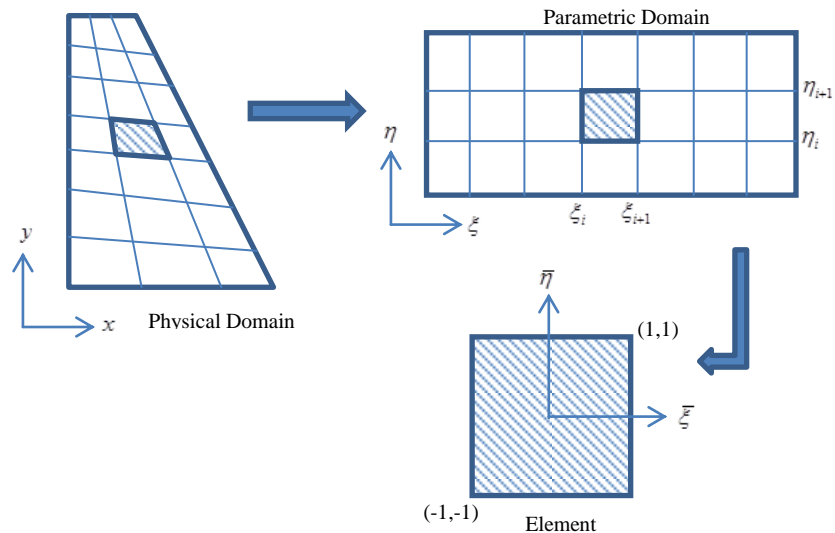


Figure 6: Relationships between different domains in IGA

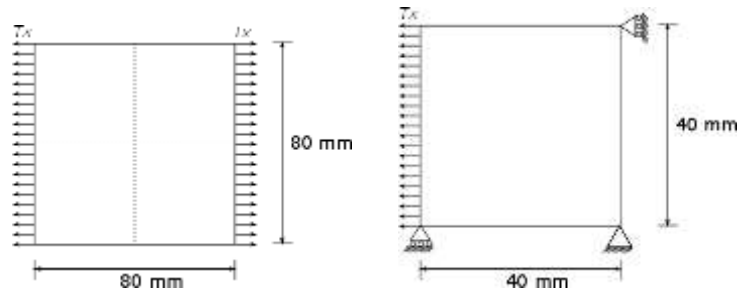


Figure 7- Square plate under uniform tension. Complete and analyzed problem

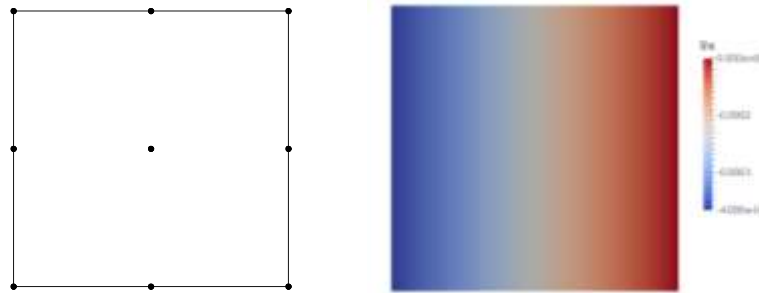


Table 1: Natural frequencies obtained for cantilever beam problem

Natural Frequencies (Hz)				
Mode	IGA (64 el)	IGA (256 el)	IGA (1024 el)	FEM (1480 el)
1	36,20	36,20	36,10	36,14
2	222,30	222,10	222,00	221,98
3	604,30	603,30	603,10	603,02
4	842,20	842,00	841,90	841,93
5	1138,60	1135,40	1135,00	1134,90
6	1799,70	1791,10	1790,30	1790,20

Table 2: Relative difference between IGA and FEM solutions

Relative Difference IGA-FEM %			
Mode	IGA (64 el)	IGA (256 el)	IGA (1024 el)
1	0,163	0,163	0,113
2	0,144	0,054	0,009
3	0,212	0,046	0,013
4	0,032	0,008	0,004
5	0,326	0,044	0,009
6	0,531	0,050	0,006

Table 3: *Vibration frequencies obtained for the dam cross section problem*

Natural Frequencies (Hz)					
Mode	FEM	IGA (192 el)	IGA(48 el)	IGA(12 el)	IGA(3 el)
1	<b>5,363</b>	5,432	5,434	5,458	5,645
2	<b>15,421</b>	15,456	15,477	15,746	18,177
3	<b>19,954</b>	19,965	19,967	19,982	20,087
4	<b>30,105</b>	30,143	30,223	31,568	36,642
5	<b>45,826</b>	45,746	45,866	46,816	49,064
6	<b>48,719</b>	48,757	48,915	52,481	69,818

Table 4: *Relative difference between IGA and FEM solutions*

Relative Difference IGA-FEM %				
FEM	IGA (192 el)	IGA(48 el)	IGA(12 el)	IGA(3 el)
1	0,771	0,798	1,070	3,160
2	0,228	0,362	2,109	17,871
3	0,054	0,063	0,142	0,668
4	0,125	0,393	4,861	21,714
5	0,175	0,086	2,159	7,067
6	0,078	0,401	7,721	43,308